Biochemistry

 Volume 39, Number 22 June 6, 2000

Accelerated Publications

Oblique Membrane Insertion of Viral Fusion Peptide Probed by Neutron Diffraction†

Jeremy P. Bradshaw,*,‡ Malcolm J. M. Darkes,‡ Thad A. Harroun,‡ John Katsaras,§ and Richard M. Epand||

Department of Preclinical Veterinary Sciences, Royal (Dick) School of Veterinary Studies, University of Edinburgh, Summerhall, Edinburgh EH9 1QH, U.K., National Research Council of Canada, Steacie Institute for Molecular Sciences, Neutron Program for Materials Research, Chalk River Laboratories, Ontario K0J 1J0, Canada, and Department of Biochemistry, McMaster University Health Sciences Centre, Hamilton, Ontario L8N 3Z5, Canada

Received February 2, 2000; Revised Manuscript Received April 17, 2000

ABSTRACT: Fusion peptides mimic the membrane fusion activities of the larger viral proteins from which they derive their sequences. A possible mode of activity involves their oblique insertion into lipid bilayers, causing membrane disruption by promoting highly curved hemifusion intermediates, leading to fusion. We have determined the location and orientation of the simian immunodeficiency virus (SIV) fusion peptide in planar lipid bilayers using neutron lamellar diffraction. The helical axis of the peptide adopts an angle of 55° relative to the membrane normal, while it positions itself nearest the lipid bilayer surface. This is the first direct observation of the structural interaction between a fusion peptide and a phospholipid bilayer.

Certain proteins have the ability to induce the fusion of two discrete phospholipid membranes (*1*). To date, the best characterized of these are derived from enveloped viruses (*2*), although there are many reports of the involvement of similar proteins in other physiological processes (*3*). Viral fusion proteins usually contain a highly conserved N-terminal region that has been shown by mutagenesis studies to be crucial to the process of fusion between the viral envelope and a membrane of the host cell during the infection process. Short peptides (10−30 residues long) with the corresponding sequence, termed fusion peptides, retain some of the membrane fusion activity of the larger protein, albeit with slower rates, and lack of a specific binding function.

The precise molecular events that occur during peptide-induced membrane fusion are still unclear. The membrane leaflets, composed of phospholipid molecules, must rearrange into highly curved intermediates prior to fusion pore development (*4*, *5*). These intermediates can be induced by peptides that increase the hydrophobic volume relative to the volume of the solvated polar groups. It has been demonstrated that peptides that lower the bilayer to the inverted hexagonal phase transition temperature in model membranes can also promote membrane fusion through this kind of bilayer destabilization.

Membrane active peptides may be classified according to their bilayer activity (*6*). In this scheme, transmembrane α-helices generally stabilize bilayers and would therefore be expected to inhibit fusion. However, certain surface-absorbed peptides are capable of bilayer destabilization, by a combination of lipid head group charge neutralization and the peptide's deep location in the bilayer.

† This work was supported by the Wellcome Trust, the BBSRC, and the National Research Council of Canada.

* To whom correspondence should be addressed: Department of Preclinical Veterinary Sciences, Royal (Dick) School of Veterinary Studies, University of Edinburgh, Summerhall, Edinburgh EH9 1QH, U.K. Fax: + 44 131 650 6139. E-mail: J.Bradshaw@ed.ac.uk.

‡ University of Edinburgh.

§ Chalk River Laboratories.

|| Mcmaster University Health Sciences Centre.

10.1021/bi000224u CCC: $19.00
Published on Web 05/11/2000

Table 1: Neutron Structure Factors Used in the Fourier Subtractions[a]

sample	*F*(1)	*F*(2)	*F*(3)	*F*(4)	*F*(5)
DOPC and SIV	−13.6(1)	−6.42(8)	3.75(4)	1.58(3)	0.83(3)
DOPC and [$^2H_8$]Val2 SIV	−15.1(1)	−7.60(8)	3.86(4)	1.53(3)	0.81(3)
DOPC and [$^2H_{10}$]Leu8 SIV	−14.8(1)	−7.50(8)	3.69(4)	−1.04(3)	0.89(3)
DOPC and [$^2H_{10}$]Leu11 SIV	−15.7(1)	−10.13(9)	5.00(6)	−2.09(3)	−1.72(3)

[a] Data were collected at 25 °C and 92% relative humidity with ^2H_2O concentrations of 0, 33, 67, and 100%. The data in the table represent 8.07% ^2H_2O, which was interpolated from the linear relationship between ^2H_2O concentration and structure factor amplitudes (*16*).

A rather different class of membrane-destabilizing peptides has been proposed by Brasseur to which viral fusion peptides are thought to belong (*7*). This model arose from analysis of the spatial distribution of hydrophobic and hydrophilic residues along the helical axis of fusion peptides. The analysis predicts an oblique insertion (55−60° relative to the bilayer normal) of the peptide that may be an initial step in membrane fusion. A correlation between predicted peptide orientation within the bilayer and fusion activity has been supported by a number of studies.

Working within Brasseur's model, Horth et al. (*8*) demonstrated that maximum fusion occurs with proteins that have obliquely inserting domains. Martin et al. designed analogues of the simian immunodeficiency virus (SIV) peptide, with a changed angle of insertion in accord with Brasseur's model, and tested them for fusion activity (*9*). Maximum fusion occurred with a calculated peptide orientation of 52°, as measured by polarized FTIR spectroscopy. However, the depth of penetration of the peptide into the bilayer could not be determined by this method.

The experiment described here is a direct observation of an obliquely inserted fusion peptide in planar phospholipid bilayers. Using neutron diffraction from stacked multilayers of 1,2-dioleoyl-*sn*-glycerophosphocholine (DOPC), we have determined, for the first time, both the bilayer location and orientation of specifically deuterated SIV fusion peptides

EXPERIMENTAL PROCEDURES

DOPC was purchased from Avanti Polar Lipids (Birmingham, AL) and used without further purification. SIV fusion peptide was synthesized and purified by Albachem (Edinburgh, U.K.) to the sequence in the Swiss Protein Data Bank: Gly-Val-Phe-Val-Leu-Gly-Phe-Leu-Gly-Phe-Leu-Ala. Four batches of the peptide were produced, one undeuterated, one deuterated at valine 2 (8 deuterons), one deuterated at leucine 8 (10 deuterons), and one deuterated at leucine 11 (10 deuterons). Twenty milligrams of DOPC and 1 mol % peptide were codissolved in chloroform/methanol and deposited by airbrush onto a silicon wafer. The wafers were placed under vacuum for 12 h to remove all traces of the solvent, before being hydrated in a humid atmosphere.

Neutron diffraction measurements were carried out on the N5 diffractometer at the NRU reactor at Chalk River Laboratories. Samples were assessed at 25 °C and 92% relative humidity. Each sample was assessed at four ^2H_2O concentrations (0, 33, 67, and 100%) to provide additional phase information. The scanning protocol consisted of sequential θ (sample angle) scans around the predicted Bragg angle for each order.

Peak fitting and background subtraction were carried out using Peakfit (Jandel Scientific Software GmbH). Absorption and Lorentz corrections were applied and the square roots

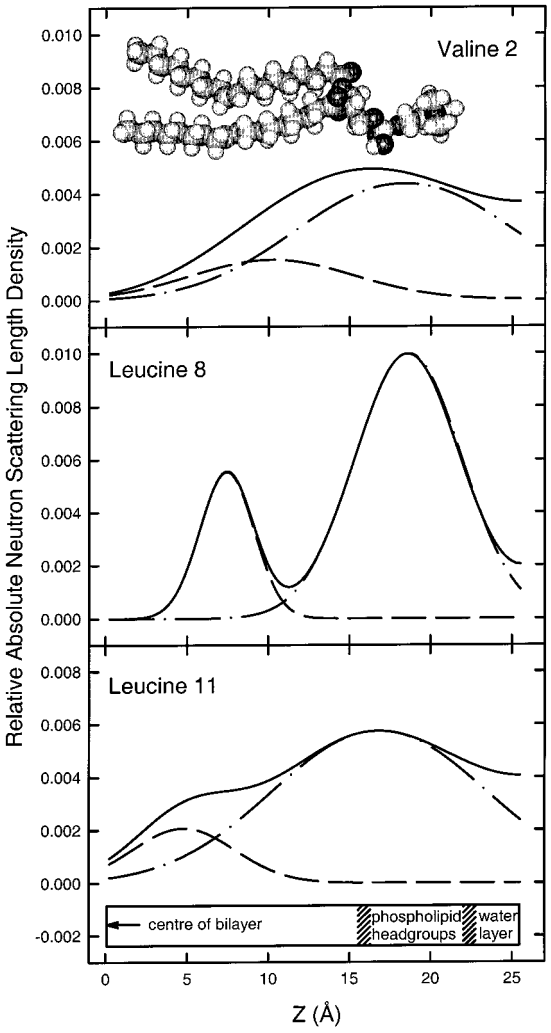

FIGURE 1: Neutron scattering length density profiles of the deuterium label in 1 mol % SIV fusion peptide in stacked multilayers of DOPC, at 25 °C and 92% relative humidity, with 8% ^2H_2O: (top) [$^2H_8$]Val2−SIV fusion peptide, (middle) [$^2H_{10}$]-Leu8−SIV fusion peptide, and (bottom) [$^2H_{10}$]Leu11−SIV fusion peptide. The profiles were calculated by fitting calculated diffraction patterns of Gaussian distributions to observed differences in neutron structure factors: (− − −) minor population of label, (−•−) major population of label, and (—) sum of major and minor populations. The structure factors for bilayers hydrated with 8% ^2H_2O were used, since water of this isotopic composition has a net neutron scattering length density of zero. The data have been scaled using the relative absolute method (*11*−*13*). Phospholipid molecules are shown above the profiles to orientate the scattering densities.

of the intensities determined to produce structure factor amplitudes. The relative scaling of the different data sets and the phases of each of their orders were determined by least-squares fitting to straight line functions. The whole procedure has been described previously (*10*). The data were placed on a "relative absolute" (*11*−*13*) scale using the

Table 2: Gaussian Models of Deuterium Label Distribution of 1.0 mol % [$^2H_{10}$]Val2−, [$^2H_{10}$]Leu8−, and [$^2H_{10}$]Leu11−SIV Fusion Peptide in Bilayers of DOPC[a]

site	parameter	valine 2	distribution	leucine 8	distribution	leucine 11	distribution
1	position[b]	19.9 ± 1.2 Å	74 ± 13%	18.6 ± 0.5 Å	76 ± 6%	16.5 ± 0.2 Å	82 ± 8%
	width[c]	7.14 ± 2.6 Å		4.6 ± 0.5 Å		8.9 ± 0.6 Å	
2	position[b]	10.5 ± 1.5 Å	26 ± 13%	7.4 ± 0.3 Å	24 ± 6%	4.8 ± 0.2 Å	18 ± 8%
	width[c]	8.67 ± 3.0 Å		2.3 ± 1.2 Å		4.5 ± 0.4 Å	
	error[d]	1.9%		1.0%		1.1%	

[a] The position, width, and size of Gaussian distributions were fitted, in reciprocal space, to difference neutron structure factors. Five orders of diffraction were used in the fitting procedure. [b] The position of each label site is expressed as the distance from the center of the bilayer. [c] The width is the full width at 1/e height. [d] The error in the Gaussian fitting procedure is expressed as the sum of the absolute differences between calculated and observed structure factors.

known neutron scattering lengths of ^2H and ^1H. This method requires knowledge of the molar percentage of water in the samples, which was determined as previously described (*14*).

RESULTS

Neutron structure factors (Table 1) were corrected, scaled, and Fourier transformed to produce neutron scattering length density profiles (data not shown). Figure 1 shows the difference in scattering density profiles between SIV peptide in DOPC and amorphously labeled (deuterated) SIV peptide in DOPC under the same sample conditions. The result shows the distribution of deuterium label across the bilayer normal. In the figure, this appears as two discrete populations for the [$^2H_{10}$]Leu8 and [$^2H_{10}$]Leu11 labels. The [$^2H_8$]Val2 label appears as a single broad peak. Gaussian distributions were fitted to these observed differences, the variables being height, width, and position along the bilayer normal. The fitting process was carried out in reciprocal (diffraction) space by comparing the calculated structure factors of each model to the observed difference structure factors. The results of the Gaussian fitting are summarized in Table 2. It should be noted that the single broad peak of the [$^2H_8$]Val2 label was also resolved into two discrete populations by this process.

All three labels clearly exhibit two discrete sites on each side of the bilayer, indicating that the SIV peptide adopts two orientations, or locations, one close to the bilayer surface and one involving insertion into the fatty acyl region. In both orientations, the N-terminus would be close to the bilayer surface, thereby explaining the overlap of the two label distributions for the [$^2H_8$]Val2 label.

Although each label has two distributions along the bilayer normal, we can still determine the orientation of the molecule unambiguously. Each scattering length density difference profile gives the time-averaged positions of all the deuterons of the labeled residue along the bilayer normal. The center of that Gaussian distribution is equivalent to the *z* value of the three-dimensional center of mass for all of the deuterons of that particular labeled residue. In other words, each label can be thought of as being centered at a point with an *x*, *y*, *z* coordinate, rather than treating each deuteron individually.

FTIR has shown that SIV fusion peptide is predominantly α-helical when associated with DOPC (*15*). However, the relatively broad peaks in the [$^2H_8$]Val2 difference profile suggest a more random structure at that terminus of the peptide. To test the Brasseur model (*7*), we assumed that the whole peptide was a rigid α-helix, knowing that we could determine the validity of its use with its goodness of fit to the data; a random secondary structure would more easily fit the data than a structurally constrained α-helix.

Table 3: Angle of the Helices of the Models in Figure 2 Relative to the Bilayer Normal[a]

major (surface) population		minor (penetrating) population	
model	angle	model	angle
A	78°	B	85°
C	55°	D	50°

[a] These were calculated by fitting a straight line to the backbone atoms to the nearest degree of tilt.

Our goal was to find the orientation of the fusion peptide such that the *z* values of the label centers coincide with the data. We began by estimating the distances between the label centers. We then assigned the following coordinates to these centers, the *z* values of which are known: (0, 0, z_1), (0, y_2, z_2), and (x_3, y_3, z_3). Using the Euclidian distances between the points from the atomic model of the protein, we have three equations and three unknowns: [y_2, x_3, y_3]. There are four solutions to these equations: [y_2, x_3, y_3], [$-y_2$, x_3, $-y_3$], [y_2, $-x_3$, y_3], and [$-y_2$, $-x_3$, $-y_3$]. Since we would expect that the peptide is free to rotate about the *z*-axis, the second and third as well as the first and fourth are equivalent orientations; therefore, there are two model solutions from which to choose for our single orientation. Clearly, a fourth label is needed to distinguish between the two models, but as we shall see, they will be different enough from each other that we can regard one as more probable than the other on the basis of other information.

In our case, since we have two *z* values for each label, there are eight possible orientations to try. Some of them will not have real solutions, meaning a physically impossible orientation. In fact, there are only two real solutions of the eight possible, which group together the measured scattering profiles very well. These solutions coincide with the relative populations of each label position, according to the area of the fitted Gaussians (see Table 2).

DISCUSSION

The result of this exercise shows a large population of peptide along the bilayer surface, and a smaller population of peptide in the hydrophobic core. For each position, we have two alternatives for the peptide's specific orientation with respect to the bilayer normal. The two possible orientations of the surface peptide are shown in parts A and C of Figure 2, and the two possible orientations of the penetrating peptide are shown in parts B and D of Figure 2. Each peptide state has an alternative that is primarily parallel to the membrane plane, and one that is oblique. There are no strictly perpendicular orientations. The alternatives are summarized in Table 3.

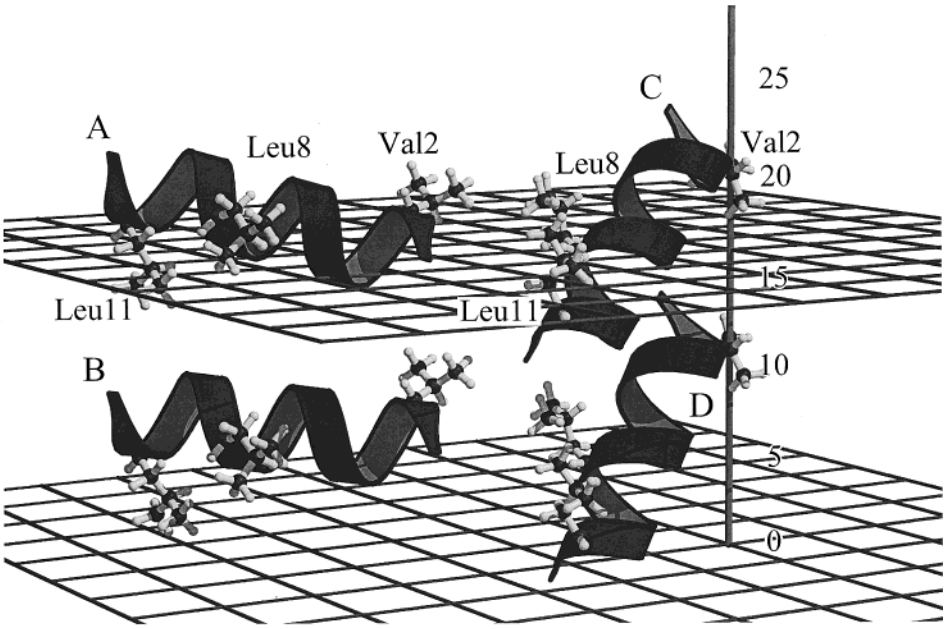

FIGURE 2: Molecular models of SIV peptide oriented in one-half of a bilayer. The vertical line is the *z*-axis scale parallel to the membrane normal. The center of the bilayer is represented by the lower mesh, and the hydrophobic and/or hydrophilic interface is suggested by the upper mesh at the approximate value of 16 Å. The peptide helix is represented as a coiled ribbon, while deuterated residues Val2, Leu8, and Leu11 are represented as a ball-and-stick model. The peptides (A and C), nearest the membrane surface, both correspond to site 1 in Table 2. These orientations are the only way to fit the data in Table 2. The authors' preference for option C is explained in the text. The figure was prepared with Molscript (*17*) and Raster3D (*18*).

It is clear, from the neutron data, that the majority of SIV fusion peptide lays close to the bilayer surface. With three labeled amino acids, it is not possible to differentiate between the two possible orientations of peptide in this location. However, when the data are interpreted in the light of previous studies, one of the alternatives becomes much more plausible than the other. One of the options, model C, has the C-terminus of the peptide penetrating into the hydrophobic core of the bilayer, as previously predicted (*7*). Moreover, the angle of this peptide, 55°, correlates closely with the predictions of this modeling work, and agrees with ATR-FTIR measurements (*9*). In contrast, the alternative interpretation of the major population has the peptide inserted at the wrong angle, and the termini are oriented in a manner that is the opposite of that predicted by other studies.

It is not straightforward to decide between the two alternatives for the minor population of peptide that is located close to the center of the bilayer. In terms of the oblique insertion model, it is the surface population with which we are most concerned, and the presence of the secondary population may well be coincidental. Indeed, it is conceivable that the secondary population is an artifact of the sample preparation technique, but we are confident that its presence does not detract from the major findings of this paper. This is because the secondary peaks also describe a specific interaction of the peptide with the bilayer. They cannot be explained, therefore, in terms of excess peptide lying randomly oriented in the fatty acyl chains of the bilayer.

In addition, it is worth noting that "top" and "bottom" sides of each peptide are defined, because the orientation about the axis of the peptide's helix is set. This means that the same residues will always face toward the center of the bilayer within the population of proteins.

We thus favor model C as the arrangement of this peptide most relevant for beginning its fusion activity. Such an orientation is in accord with several experimental and theoretical observations. The peptide is shown by our work to have an angle of insertion into the membrane similar to that found by polarized FTIR. The only charged group, when the carboxyl group is blocked by extension of the protein, is the terminal amino group. This mode of insertion avoids placing the amino group in a hydrophobic environment in the membrane.

Fusion peptides play an important role in viral fusion. Their location in viral fusion peptides has been indicated by loss of viral infectivity when positions within this region are mutated and by the fact that isolated synthetic peptides corresponding to these segments of the protein are perturbing with respect to membranes. The exact manner in which they alter the properties of membranes to facilitate the formation of fusion intermediates is currently an area of active research. The oblique mode of insertion of fusion peptides as α-helices has been correlated with the ability of this peptide to increase negative membrane curvature. The formation of the first hemifusion intermediate is promoted by membrane negative curvature. Our findings therefore provide unique direct evidence for the nature of the insertion of the SIV fusion peptide into membranes. The suggested mode of insertion also leads naturally to the proposal that a likely consequence of this insertion is the destabilization of membrane bilayers.

ACKNOWLEDGMENT

We thank Jean-Marie Ruysscheart for helpful discussions.

REFERENCES

1. White, J. M. (1992) *Science 258*, 917.
2. Hughson, F. M. (1997) *Curr. Biol. 7*, R565.
3. Bennett, M. K., and Scheller, R. H. (1994) *Annu. Rev. Biochem. 63*, 63.
4. Siegel, D. P. (1999) *Biophys. J. 76*, 291.

5. Spruce, A. E. (1994) *Proc. Natl. Acad. Sci. U.S.A. 88*, 3623.
6. Epand, R. M. (1995) *Biopolymers 37*, 319.
7. Brasseur, R., Vandenbranden, M., Cornet, M., Burny, A., and Ruysschaert, J. (1990) *Biochim. Biophys. Acta 1029*, 267.
8. Horth, M., Lambrecht, V., Chuan Lay Kim, M., Bex, F., Thiriart, C., Russchaert, J.-M., Burny, A., and Brasseur, R. (1991) *EMBO J. 10*, 2747.
9. Martin, I., Dubois, M.-C., Defrise-Quertain, F., Saermark, T., Burny, A., Brasseur, R., and Russchaert, J.-M. (1994) *J. Virol. 68*, 1139.
10. Duff, K. C., Gilchrist, P. J., Saxena, A. M., and Bradshaw, J. P. (1994) *Virology 202*, 287.
11. Wiener, M. C., King, G. I., and White, S. H. (1991) *Biophys. J. 62*, 2762.
12. Wiener, M. C., and White, S. H. (1991) *Biophys. J. 59*, 162−185.
13. Jacobs, R. E., and White, S. H. (1989) *Biochemistry 28*, 3421.
14. Bradshaw, J. P., Davies, S. M. A., and Hauss, T. (1998) *Biophys. J. 75*, 889.
15. Martin, I., Defrise-Quertain, F., Mandieau, V., Nielsen, N. M., Saermark, T., Burny, A., Brasseur, R., Russchaert, J.-M., and Vandenbranden, M. (1991) *Biochem. Biophys. Res. Commun. 175*, 872−879.
16. Darkes, M. J. M., and Bradshaw, J. P. (2000) *Acta Crystallogr. Sect. D 56*, 48−54.
17. Kraulis, P. J. (1991) *J. Appl. Crystallogr. 24*, 946.
18. Merritt, E. A., and Bacon, D. J. (1997) *Methods Enzymol. 277*, 505.

BI000224U